A Letters Journal Exploring the Frontiers of Physics

May 2008

EPL, **82** (2008) 34002
doi: 10.1209/0295-5075/82/34002

www.epljournal.org

Directional emission from an optical microdisk resonator with a point scatterer

C. P. Dettmann[1], G. V. Morozov[1], M. Sieber[1] and H. Waalkens[1,2(a)]

[1] *First Institute, Department of Mathematics, University of Bristol - Bristol BS8 1TW, UK, EU*
[2] *Second Institute, Department of Mathematics, University of Groningen - Nijenborgh 9, 9747 AG Groningen, The Netherlands, EU*

received 22 November 2007; accepted in final form 10 March 2008
published online 18 April 2008

PACS 42.55.Sa – Microcavity and microdisk lasers
PACS 42.25.-p – Wave optics
PACS 05.45.Mt – Quantum chaos; semiclassical methods

Abstract – We present a new design of dielectric microcavities supporting modes with large quality factors and highly directional light emission. The key idea is to place a point scatterer inside a dielectric circular microdisk. We show that, depending on the position and strength of the scatterer, this leads to strongly directional modes in various frequency regions while preserving the high Q-factors reminiscent of the whispering gallery modes of the microdisk without scatterer. The design is very appealing due to its simplicity, promising a cleaner experimental realisation than previously studied microcavity designs on the one hand and analytic tractability based on Green's function techniques and self-adjoint extension theory on the other.

Introduction. – Modern fabrication techniques enable the construction of dielectric optical resonators on a microscopic scale. Light is trapped by utilizing the principle of total internal reflection. These microcavities have great potential for a wide range of applications and studies in laser physics and microphotonics [1,2], like the realization of miniature laser sources, the creation of dynamical filters for optical communications and the suppression and enhancement of spontaneous emission.

For many practical purposes it is crucial to have microcavities that possess resonances with long lifetimes (which is a prerequisite for low threshold lasing) and highly directional emission patterns. The lifetimes are characterized by the so-called Q-factor given by $Q=\omega/\Delta\omega$, where $\omega-\mathrm{i}\Delta\omega/2$ is the complex frequency of the resonance with $\Delta\omega$ being the linewidth or inverse lifetime. The best known example of modes with high Q-factors are the so-called whispering gallery modes (WGMs) which are the optical analogues of the acoustic waves evolving along the walls of convex-shaped halls first studied by Lord Rayleigh in the 19th century. The experimental realization of a thin microdisk laser based on WGMs was first reported in [3]. Theoretical studies [4] show that the WGMs of an ideal circular microcavity can lead to very high Q-factors of the order 10^6–10^{13}. Despite a significant degradation due to imperfections on the disk boundary, inhomogeneity of the refractive index inside the disk, effects of coupling to the substrate etc., typical experimental Q-factors of the dielectric-disk resonances remain quite high, usually $\approx 10^4$, with the record value of $Q\approx 5\times 10^5$ [5]. However, the applicability of circular microdisk lasing cavities is limited by their isotropic light emission. In order to obtain a directional optical output one has to break the rotational symmetry, for example, by deforming the boundary of the cavity [6–12]. This significantly improves the emission directionality but typically spoils the Q-factors. Moreover, in many cases this approach leads to more than one angular emission peak in the far-field region [7,8].

Another approach to breaking the symmetry is to insert an obstacle like a linear defect [13,14] or a hole [15] into the microdisk. This indeed allows one to obtain resonances with very large Q-factors and relatively high unidirectional emission pattern in the far-field region. It has also been shown that it is possible to obtain directional emission from either undeformed microspheres [16,17] or undeformed microdisks [5] by coupling light into and out of them with the aid of an optical fiber taper waveguide. A thorough review of this technique has been recently given in [18]. However, the systems mentioned above often require quite extensive numerics like various modifications

(a) E-mail: H.Waalkens@rug.nl

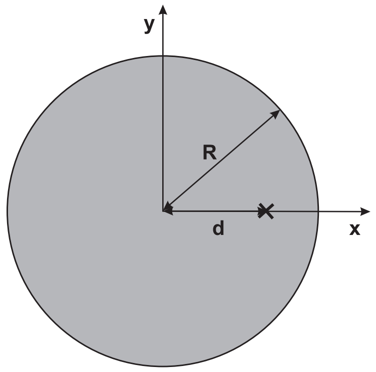

Fig. 1: Microcavity of refractive index n and radius R with a point scatterer at the distance d from the center. The external medium has refractive index $n_{\rm ext}=1$.

of the boundary element method [19,20] or the S-matrix approach [4,21] to find resonances and optimize design parameters.

In this letter, we propose a much simpler method which significantly improves directionality of the modes of conventional microdisk resonators while keeping their Q-factors high ($>10^4$). The symmetry is broken by placing a point scatterer within the inner region of the microdisk, see fig. 1. It turns out that such a geometry improves the emission directionality of microdisk modes for a wide range of frequencies, especially in the visible spectrum. Moreover, this approach is to a large extent analytically tractable enabling a systematic optimization of the design parameters (location and strength of the scatterer) with only modest numerical effort.

Closed systems with a point scatterer have been extensively studied in the context of "quantum chaos" [22] showing that the spectral properties of such systems can be obtained from self-adjoint extension theory [23]. Similarly to the case of closed systems, it turns out that the resonance wave functions of the open microdisk with a point scatterer are essentially given by the Green's function of the microdisk without scatterer (unperturbed microdisk).

Unperturbed microdisks. – If we treat a microcavity as a passive object, we can find its resonances from Maxwell's equations with a refractive index independent of the EM field. In general, a microcavity is a 3D object and, as a result, resonant modes have all 6 EM field components. However, for a zero axial momentum EM field, *i.e.* for waves with $k_z=0$, where z is perpendicular to the disk plane $(x,\,y)$, a thin passive microdisk can be modeled as a 2D dielectric disk of radius R, with the effective refractive index $n_{\rm eff}(r)=n$, which takes into account the material as well as the thickness of the microdisk. In this model, Maxwell's equations reduce to two scalar Helmholtz equations corresponding to TM and TE polarizations, respectively, with each polarized mode having just three EM field components. For brevity we consider only TM modes in this paper. However, the study of TE resonant modes is also relevant for the design of functional microlasers. In particular the effective refractive index of a thin slab could be larger for those modes than for TM modes [24].

The electric field of TM modes is of the form $\mathbf{E}=E_z(x,y)\,\mathbf{e}_z$, and for a wave number $k=\omega/c$, E_z satisfies the Helmholtz equation $[\nabla^2+k^2n^2(r)]E_z=0$, where $n(r)=n$ if $r<R$, and $n(r)=n_{\rm ext}=1$ if $r>R$. Due to circular symmetry this equation can be separated in polar coordinates (r,ϕ) where the TM modes are then characterized by azimuthal and radial modal indices $m=0,\pm1,\pm2,\dots$ and $q=1,2,3,\dots$, respectively. Following [25], we seek the Green's function in the form

$$G(\mathbf{r},\mathbf{r}_0,k)=\sum_{m=-\infty}^{\infty}\frac{e^{im(\varphi-\varphi_0)}}{2\pi r_0 W}E_1(r_<,k)E_2(r_>,k),$$

where $E_{1,2}(r)$ are solutions of the homogeneous equation

$$\left(r^2\frac{d^2}{dr^2}+r\frac{d}{dr}+k^2n^2(r)r^2-m^2\right)E\,(r)=0,$$

$W=W(E_1,E_2)$ is the Wronskian evaluated at r_0, and $r_<$ ($r_>$) is the smaller (respectively larger) of r and r_0. The physical boundary conditions require $E_1(r)$ to be finite at $r=0$ and $E_2(r)$ to be an outgoing wave for $r\to\infty$. Requiring $E_{1,2}$ to be smooth at $r=R$ then leads to

$$G(\mathbf{r},\mathbf{r}_0,k)=-\frac{i}{4}H_0\,(kn\,|\mathbf{r}-\mathbf{r}_0|)+\frac{i}{4}\sum_{m=0}^{\infty}\frac{C_m}{A_m}\epsilon_m\cos\left[m\,(\varphi-\varphi_0)\right]J_m\,(knr_<)\,J_m\,(knr_>),\tag{1}$$

if both $r_<$ and $r_>$ lie inside the disk of radius R,

$$G(\mathbf{r},\mathbf{r}_0,k)=\frac{1}{2\pi kR}\sum_{m=0}^{\infty}\frac{1}{A_m}\epsilon_m\cos\left[m\,(\varphi-\varphi_0)\right]J_m(knr_<)H_m(kr_>),\tag{2}$$

if $r_<<R$ and $r_>>R$, and, finally,

$$G(\mathbf{r},\mathbf{r}_0,k)=-\frac{i}{4}H_0\,(k\,|\mathbf{r}-\mathbf{r}_0|)+\frac{i}{4}\sum_{m=0}^{\infty}\frac{B_m}{A_m}\epsilon_m\cos\left[m\,(\varphi-\varphi_0)\right]H_m(kr_<)H_m(kr_>),\tag{3}$$

if both $r_<$ and $r_>$ lie outside the disk of radius R. The coefficients are $\epsilon_m=2$ if $m\neq0$, $\epsilon_m=1$ if $m=0$, and

$$A_m=J_m(knR)H'_m(kR)-nJ'_m(knR)H_m(kR),$$
$$B_m=J_m(knR)J'_m(kR)-nJ'_m(knR)J_m(kR),$$
$$C_m=H_m(knR)H'_m(kR)-nH'_m(knR)H_m(kR).$$

The functions J_m and H_m are Bessel and Hankel functions of the first kind, respectively. The resonances $k_{\rm res}$ of the microdisk are determined by the poles of the Green's function which are given by $A_m=0$, *i.e.*

$$J_m(k_{\rm res}nR)H'_m(k_{\rm res}R)-nJ'_m(k_{\rm res}nR)H_m(k_{\rm res}R)=0.$$

Resonances differing by the sign of m are degenerate.

Microdisks with a point scatterer. – The Green's function (1) is logarithmically divergent at the point $\mathbf{r} = \mathbf{r}_0 = \mathbf{d}$ where $d < R$, since

$$H_0(z) = 1 + \frac{2\mathrm{i}}{\pi}\left(\ln z + \gamma - \ln 2\right) + \mathcal{O}(z^2),$$

where $\gamma = 0.5772\ldots$ is the Euler-Mascheroni constant. The regularized Green's function G_r can be obtained from (1) if we subtract the term $\ln(k_0|\mathbf{r} - \mathbf{r}_0|)/2\pi$, where k_0 is an arbitrary constant. It then follows from the self-adjoint extension theory [23] that the resonances k_res of the microdisk with a point scatterer at position $\mathbf{d}$ and of coupling strength λ satisfy the condition [26]

$$0 = 1 - \lambda G_\mathrm{r}(\mathbf{d}, \mathbf{d}, k_\mathrm{res}), \qquad (4)$$

where $G_\mathrm{r}(\mathbf{d}, \mathbf{d}, k)$ is the regularized Green's function at the point $\mathbf{r} = \mathbf{r}_0 = \mathbf{d}$. Note that our regularization of the Green's function differs from the one given in eq. (14) of [26]. In general, regularizations can differ by an additive real constant. This is compensated by a redefinition of the coupling parameter λ, see also the discussion in sect. 3 of [27]. It is convenient to introduce the new coupling parameter a which is defined by $2\pi/\lambda \equiv -\ln(k_0 a)$. Equation (4) then reads

$$0 = -\frac{\mathrm{i}}{4} + \frac{1}{2\pi}\left(\ln\frac{k_\mathrm{res} n a}{2} + \gamma\right) + \frac{\mathrm{i}}{4}\sum_{m=0}^{\infty}\frac{C_m}{A_m}\epsilon_m J_m^2\left(k_\mathrm{res} n d\right).$$

Following ideas similar to those in [28], it is not difficult to show that the parameter a can be identified with the radius of a finite-size perturbation of refractive index n_p in the limit $kna \ll 1$ when $n_p \gg n$.

The resonance wave functions $E_z(\mathbf{r}, k_\mathrm{res})$ are given by

$$E_z\left(\mathbf{r}, k_\mathrm{res}\right) = N\, G\left(\mathbf{r}, \mathbf{d}, k_\mathrm{res}\right), \qquad (5)$$

where $G(\mathbf{r}, \mathbf{d}, k_\mathrm{res})$ is the unregularized Green's function (1) and N is a normalization factor.

Note that m is no longer a good modal index of the microdisk with a point scatterer. However, it follows from condition (4) that for a vanishing strength of the point scatterer ($\lambda \to 0\pm$ or equivalently $a = 0$ or $a = +\infty$) the resonances of the microdisk with scatterer coincide with those of the unperturbed microdisk, which, for $m \neq 0$, are twofold degenerate. In fact, if the coupling parameter a varies from 0 to $+\infty$ one of the members of each pair of degenerate resonances remains unchanged. The other member is moving in the complex-k plane along a line segment that connects two resonances of the unperturbed microdisk. This can be understood from the fact that for a vanishing strength of the scatterer the angular dependence of the resonant modes is given by $\sin(m\varphi)$ and $\cos(m\varphi)$. The unperturbed resonance is the one with a nodal line along the x-axis on which we place the scatterer (see fig. 1), *i.e.* the resonance with the angular part $\sin(m\varphi)$.

In case of 3D microspheres, a similar effect of splitting initially degenerate $+m$ and $-m$ WGM resonances due to scattering on material inhomogeneities, was first observed in [29] and later addressed in more detail in [30], where a model of weak scattering by randomly distributed point-like defects was used. In contrast to that model, the scattering in our case is due to a single point-like defect which can also be relatively strong. Arguments based on geometric optics [31] predict that the highest Q values correspond to modes concentrated at the resonator edge (high m); this is in fact observed for both microspheres and also our microdisk (see figs. 2 and 3, and the discussion below).

We study the dynamics of the resonances upon varying the coupling parameter a for a typical GaAs microdisk of effective refractive index $n = 3$ and radius $R = 1\,\mu$m [32], with a point scatterer placed at three different distances ($0.99\,\mu$m, $0.495\,\mu$m, $0.25\,\mu$m) from the center of the disk. Figures 2 and 3 show the corresponding resonances in the frequency regions $\nu = c\mathrm{Re}(k)/2\pi = 0.095 - 1.050 \times 10^{14}$ Hz (mid infrared) and $\nu = 5.777 - 6.016 \times 10^{14}$ Hz (green light), respectively. Interestingly, the line segments parametrized by the coupling parameter a do not only connect different resonances of the unperturbed microdisk but as indicated in the insets in fig. 2 and in fig. 3 there are also loops connecting single resonances to themselves.

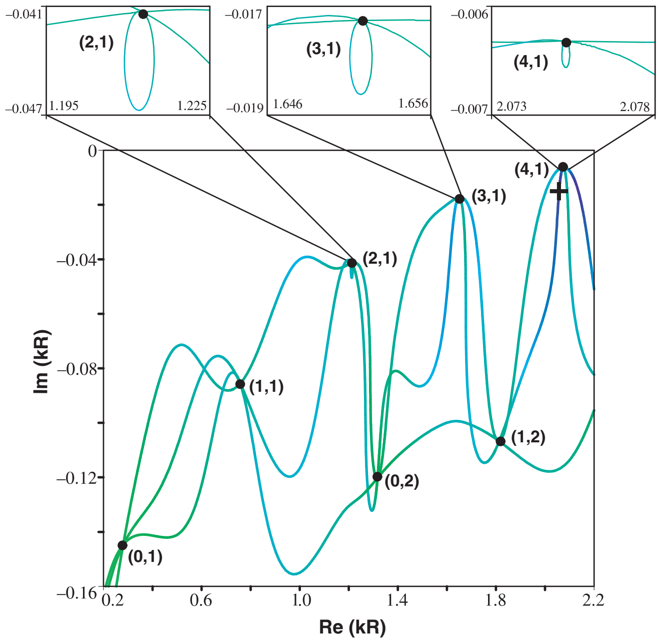

Fig. 2: (Color online). Level dynamics of the resonances in the complex wave number plane for a dielectric disk with $n = 3.0$ and $R = 1\,\mu$m and a point scatterer of varying coupling parameter a. The circles mark the unperturbed resonances with azimuthal and radial modal indices (m, q). For the upper curve the scatterer has distance $d = 0.99\,\mu$m from the center, for the middle curve $d = 0.495\,\mu$m, and for the lower curve $0.25\,\mu$m. The color code indicates the directivity D of the emission (green marks small values of D, red marks high values of D). The cross corresponds to the HD mode ($D = 5.89$, $Q = 63$) with $kR = 2.0571 - \mathrm{i}\,0.0164$ ($d = 0.495\,\mu$m, $a \approx 0.754$).

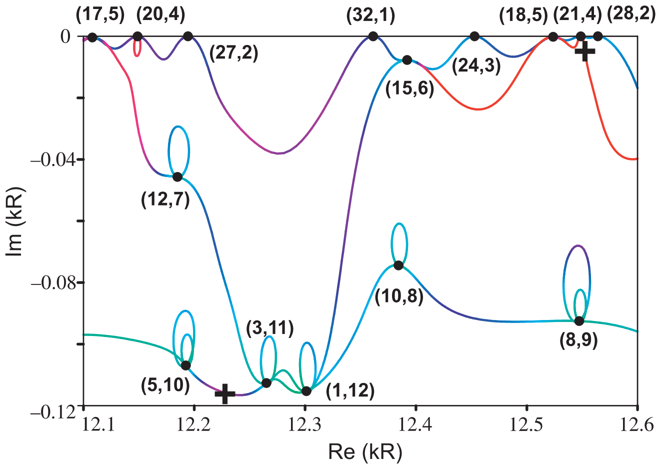

Fig. 3: (Color online). Continuation of fig. 2 for a different frequency range. The lower cross corresponds to the HD mode ($D = 7.44$, $Q = 53$) with $kR = 12.2257 - \mathrm{i}\,0.1156$ ($d = 0.25\,\mu$m, $a \approx 0.047$). The upper cross corresponds to the HD mode ($D = 14.25$, $Q = 15400$) with $kR = 12.5501 - \mathrm{i}\,0.0004$ ($d = 0.495\,\mu$m, $a \approx 0.0005$).

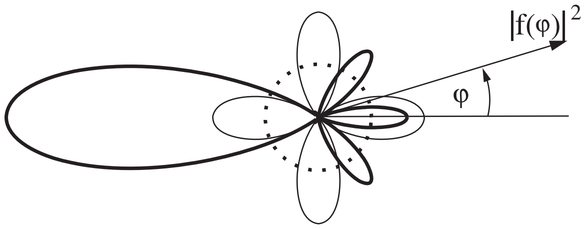

Fig. 4: Polar plot of the far-field intensity $|f(\varphi)|^2$ for the unperturbed resonant mode $(0,1)$ (dashed circle), the unperturbed resonant mode $(2,1)$ (thin solid line), and the HD perturbed resonant mode marked by the cross in fig. 2 (thick solid line). The parameters are the same as in fig. 2.

In order to quantify the far-field directionality of the electric field we consider its asymptotic behaviour for $r \to \infty$ which has the form

$$E_z(\mathbf{r}, k_{\mathrm{res}}) = E_z(r, \varphi, k_{\mathrm{res}}) \propto \frac{\exp(\mathrm{i} k_{\mathrm{res}} r)}{\sqrt{r}} f(\varphi).$$

To characterize the directionality we compute the directivity of the far-field intensity

$$D = \frac{2\pi\, |f_{\max}(\varphi_{\max})|^2}{\int_0^{2\pi} |f(\varphi)|^2 \,\mathrm{d}\varphi}.$$

From this definition it follows that $D = 1$ and $D = 2$ for resonances which have $m = 0$ and $m \neq 0$, respectively, for $a = 0$ or $a = \infty$.

In figs. 2 and 3 the directivity D is indicated by color in the range from light green (low directional modes) through blue and violet to deep red (highly directional modes). It reaches values as high as $D \approx 15$ for some specific modes. We see that there are highly directional modes (HD) for

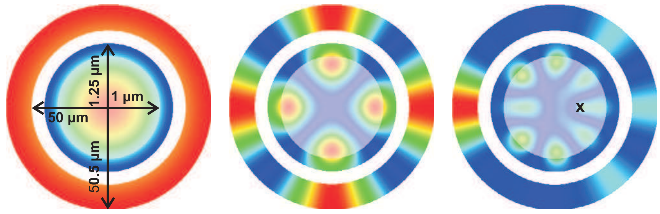

Fig. 5: (Color online). The intensity of the electric field in near- and far-field regions for unperturbed resonant modes $(0,1)$ (left), $(2,1)$ (middle), and for the HD perturbed resonant mode marked by the cross in fig. 2 (right). The parameters are the same as in fig. 2.

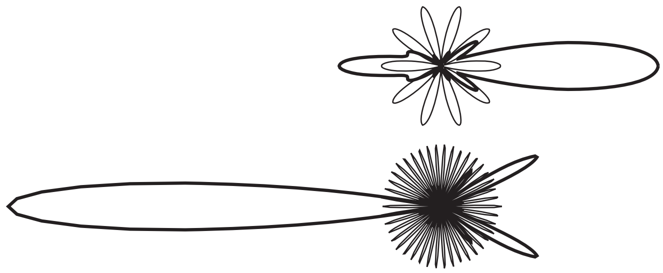

Fig. 6: Polar plot of the far-field intensity $|f(\varphi)|^2$ for the unperturbed resonance with modal indices $(m,q) = (5,10)$ (thin solid line in the top panel), the HD perturbed resonant mode marked by the lower cross in fig. 3 (thick solid line in the top panel), the unperturbed resonance with $(m,q) = (21,4)$ (thin solid line in the bottom panel), the HD perturbed resonant mode marked by the upper cross in fig. 3 (thick solid line in the bottom panel). The parameters are the same as in fig. 3.

a wide range of Q-factors which in terms of the complex wave numbers k are given by $Q = -\mathrm{Re}(k)/(2\,\mathrm{Im}(k))$.

To illustrate the directivity in more detail we compute in fig. 4 the function $|f(\phi)|^2$ for two unperturbed resonant modes and one perturbed HD mode in the frequency region of fig. 2. The corresponding near- and far-field electric-field intensities are shown in fig. 5. For a vanishing coupling strength the angular dependence is sinusoidally modulated with the number of minima being given by twice the modal index m, *i.e.* only for $m = 0$ the emission is strictly isotropic. The radial modal index q determines the number of minima in the radial direction.

Figures 6 and 7 show the near- and far-field electric-field intensities for two perturbed HD modes in the higher frequency region of fig. 3. This demonstrates that these can differ significantly from the nearby modes of the unperturbed system also shown in fig. 6. While the near-field pattern of the mode shown in the right panel of fig. 7 is still reminiscent of a WGM, the mode in the left panel is strongly scarred. The far-field patterns shown in figs. 6 and 7 also show that the scatterer can cause directional output in either direction of the symmetry axis. The mode in the bottom panel of fig. 6 has both extremely high directivity and a very high Q-factor. From fig. 3 we see that there is quite a broad spectral range of green light

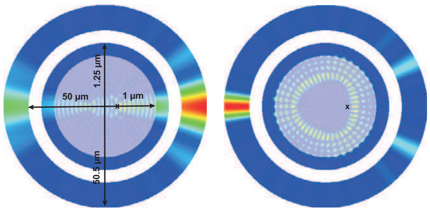

Fig. 7: (Color online). The intensity of the electric field in near- and far-field regions for HD perturbed resonant mode shown by the lower cross in fig. 3 (left) and for the HD perturbed resonant mode marked by the upper cross in fig. 3 (right). The parameters are the same as in fig. 3.

with these properties the realization of which is a major goal in semiconductor physics.

Conclusions. – In summary, we presented theoretical results that demonstrate the existence of highly directional TM modes in the emission spectrum of a microdisk cavity with a point scatterer. Though the interpretation of the coupling parameter a as the radius of a finite-size circular scatterer is strictly valid only in the limit of a small scatterer with a high refractive index, it is important to note that the results presented appear to be very robust. In particular, the form of the resonance wave function (5) holds for any small perturbation that can be treated in the s-wave approximation. This independence of the details of the scatterer has the potential to facilitate a relatively simple experimental realization.

The level dynamics of the resonances upon varying the coupling parameter is of theoretical interest in its own right and deserves further investigation. It would be also interesting to get a deeper insight into the output emission directionality by relating the resonance wave functions to the underlying ray dynamics in the semiclassical limit.

REFERENCES

[1] Vahala K. J., *Nature*, **424** (2003) 839.
[2] Ilchenko V. S. and Matsko A. B., *IEEE J. Sel. Top. Quantum Electron.*, **12** (2006) 15.
[3] McCall S. L., Levi A. F. J., Slusher R. E., Pearton S. J. and Logan R. A., *Appl. Phys. Lett.*, **60** (1992) 289.
[4] Rahachou A. I. and Zozoulenko I. V., *Appl. Opt.*, **43** (2004) 1761.
[5] Borselli M., Srinivasan K., Barclay P. E. and Painter O., *Appl. Phys. Lett.*, **85** (2004) 3693.
[6] Levi A. F. J., Slusher R. E., McCall S. L., Pearton S. J. and Logan R. A., *Appl. Phys. Lett.*, **62** (1993) 561.
[7] Nöckel J. U., Stone A. D. and Chang R. K., *Opt. Lett.*, **19** (1994) 1693.
[8] Nöckel J. U., Stone A. D., Chen G., Grossman H. L. and Chang R. K., *Opt. Lett.*, **21** (1996) 1609.
[9] Nöckel J. U. and Stone A. D., *Nature*, **385** (1997) 45.
[10] Gmachl C., Capasso F., Narimanov E. E., Nöckel J. U., Stone A. D., Faist J., Sivco D. L. and Cho A. Y., *Science*, **280** (1998) 1556.
[11] Lebental M., Lauret J. S., Hierle R. and Zyss J., *Appl. Phys. Lett.*, **88** (2006) 031108.
[12] Lee S. B., Yang J., Moon S., Lee J. H., An K., Shim J. B., Lee H. W. and Kim S. W., *Appl. Phys. Lett.*, **90** (2007) 041106.
[13] Apalkov V. M. and Raikh M. E., *Phys. Rev. B*, **70** (2004) 195317.
[14] Tulek A. and Vardeny Z. V., *Appl. Phys. Lett.*, **90** (2007) 161106.
[15] Wiersig J. and Hentschel M., *Phys. Rev. A*, **73** (2006) 031802(R).
[16] Knight J. C., Cheung G., Jacques F. and Birks T. A., *Opt. Lett.*, **22** (1997) 1129.
[17] Gorodetsky M. L. and Ilchenko V. S., *J. Opt. Soc. Am. B*, **16** (1999) 147.
[18] Srinivasan K. and Painter O., *Phys. Rev. A*, **75** (2007) 023814.
[19] Wiersig J., *J. Opt. A: Pure Appl. Opt.*, **5** (2003) 53.
[20] Boriskina S. V., Sewell P., Benson T. M. and Nosich A. I., *J. Opt. Soc. Am. A*, **21** (2004) 393.
[21] Hentschel M. and Richter K., *Phys. Rev. E*, **66** (2002) 056207.
[22] Šeba P., *Phys. Rev. Lett.*, **64** (1990) 1855.
[23] Zorbas J., *J. Math. Phys.*, **21** (1980) 840.
[24] Frateschi N. C. and Levi A. F. J., *Appl. Phys. Lett.*, **66** (1995) 2932.
[25] Morse P. M. and Feshbach H., *Methods of Theoretical Physics, Part I* (McGraw-Hill, New York) 1953.
[26] Shigehara T., *Phys. Rev. E*, **50** (1994) 4357.
[27] Sieber M., *Nonlinearity*, **20** (2007) 2721.
[28] Exner P. and Šeba P., *Phys. Lett. A*, **222** (1996) 1.
[29] Gorodetsky M. L. and Ilchenko V. S., *Laser Phys.*, **2** (1992) 1004.
[30] Weiss D. S., Sandoghdar V., Hare J., Lefêvre-Seguin V., Raimond J.-M. and Haroche S., *Opt. Lett.*, **20** (1995) 1835.
[31] Gorodetsky M. L., Pryamikov A. D. and Ilchenko V. S., *J. Opt. Soc. Am. B*, **17** (2000) 1051.
[32] Peter E., Senellart P., Martrou D., Lemaître A., Hours J., Gérard J. M. and Bloch J., *Phys. Rev. Lett.*, **95** (2005) 067401.